Discussion of sources of error in laser-speckle based systems

Bernhard G. Zogar

Institute for Measurement Technology, Johannes Kepler University, Altenbergerstraße 69, 4040 Linz, Austria

Corresponding author: bernhard.zagar@jku.at

Received December 9, 2010; accepted January 28, 2011; posted online May 18, 2011

Applying laser-speckle techniques in material sciences as well as in methods to characterize surface conditions of specimen has become the method of choice, especially if a non-contacting principle is sought. This is almost always the case for specimen that are small in at least one dimension as for example in the material testing of foils, fibres, or micromaterials and certainly also if elevated test-temperatures are preventing standard gauges. This letter discusses in some detail sources of error that are quite often overlooked or not even considered as significant at all, but still carry the potential to introduce uncertainties well above the system design specifications.

OCIS codes: 120.6165, 120.3940

doi: 10.3788/COL201109.071203.

Speckles in general and laser speckles in particular are rather interesting phenomena in optics as well as in measurement technology, since they are able to convey significant information about properties of the illuminated surface of the reflector. Speckles, most of the time causing deteriorating effects, are experienced in systems utilizing highly coherent laser[1−3], in systems where acoustic wave phenomena are studied like in ultrasonic imaging systems[4] and also in radar systems where the coherent processing of tightly phase-locked but spread in time pulses is necessary to obtain so-called synthetic imaging radar views[5].

In material science applications, most laser-induced speckles are considered and most of the time one is interested in mechanical deformation parameters. Some of the well-known non-contacting methods for measuring mechanical strain within specimen or measuring displacements of specimen surface elements (to subsequently determine some mechanical properties of the specimen) rely on the information on surface element positions conveyed by these laser-speckles. Speckles only seen when coherent wave phenomena are investigated are caused by waves scattered off of typically rough surfaces interfering in the observers, eyes or at the face plate of a camera used. The speckle pattern appears and actually is random but still bears a deterministic relationship to the scattering surfaces, optical properties just as if it were an optical fingerprint of that surface itself. It therefore seems clear that research has been put forward to utilize the information content of speckles in various contexts[6−10]. Most theoretical treatments on possible applications of speckles[1,6,7] do not cover influences that might result in measurement errors not directly linked to the speckle effect itself but dependent on the refractive index of air, the quality of the laser beam used to illuminate the specimen, etc.

In this letter, some widely overlooked sources of errors that, if unavoidable, increase measurement uncertainty beyond the theoretical limit attainable are discussed, and the magnitude of their influence is detailed. In particular, the following effects are considered: the laser-source wavelength stability as well as its pointing stability, the effects caused by so-called schlieren occuring along the optical path as well as temperature effects causing changes in the systems geometry, thermally influencing the optical parameters of the imaging optics as well as the often overlooked and in most illumination systems unknown radius of curvature of the laser wavefronts used to illuminate the specimen.

Small though as these influences seem, they might contribute significant uncertainties especially in material testing applications where the strain $\varepsilon = \frac{\Delta\ell}{\ell}$ is to be determined out of consecutive measurements of usually small changes in overall length ℓ of the specimens geometry parameter. Typical values of ε are bounded by $\pm 2,000$ ppm (the typical range of Hooke's law for steel). So values of $\Delta\ell$ on the order of tenth of micrometers for typical gauge lenghts around 50 mm yield ppm resolutions for ε. Analyzing the above mentioned error sources, one can quickly see that all of them, if not taken care of appropriately, carry the potential to cause significantly larger deviations than the resolution sought after demands.

To show the deteriorating effects of influences on speckles (a typical speckle pattern is shown in Fig. 1) listed above, a typical application is used as an example. One particular application that is to be considered in this contribution is the measurement of mechanical strain $\varepsilon = (x_\mathrm{a} - x_\mathrm{b})/\ell$ via the determination of the mechanical or thermal stress induced displacements x_a and x_b of two geometrically separated surface elements (A and B)
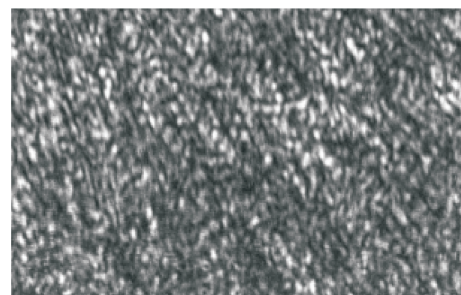

Fig. 1. A typical laser-speckle pattern as scattered off of an optically rough surface.
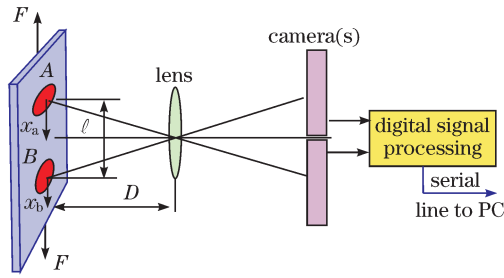
Fig. 2. Optical set-up of a speckle-correlation based strain measurement system. Two lasers illuminate two distinct spots (A and B) on the specimen surface generating speckles that are imaged by the optics (lens) and projected onto the face plate of a single or two (as indicated) charge-coupled device (CCD) cameras. Stress causes the displacement of the surface underneath the fixed in space laser spots giving rise to equivalent, since caused by the surface roughness-motions of the associated speckles that is recorded by the camera and processed further to give strain.

divided by the initial distance ℓ of the surface elements centers as is shown in Fig. 2. Figure 3 shows an actual realization of such a system that is able to resolve displacement magnitudes down to 100 nm given those error sources discussed below are tightly kept in check. This resolution is independent of the type of pattern matching or pattern tracking algorithm utilized[11] in the digital signal/image processing stage and is-assuming the processing is ideal, as will be shown limited by imponderables of the overall system.

So far only the working principle of one particular realization of a measurement system has been explained without any reference to the system pattern tracking algorithm which is of no concern here and assumed to work perfectly. In this letter, only often overlooked error contributions are considered that might degrade performance but are usually not even considered by system users who typically blame the manufacturer for not providing a stable enough system.

Most people recognize schlieren[12] as the light refracting action due to thermally induces density variations in the atmosphere typically seen close to lit candles, a typical one displayed in Fig. 4, where a gas plume from an unlit cigarette lighter is imaged[13]. The schlieren system sensitivity set to be able to image the gas plume is around $10''$ for maximum brightness. A number that might be considered negligible at a first glance for measurement systems. If, however, one is taking the actual imaging geometry of a speckle system into account where typical lenghts of the optical path are around 300 mm and temperature gradients over the specimens vertical extension might be a few K or even more the deviation form a straight line propagation of light might be signifcant.

Following Ref. [12], the refractive index of air n_{air} is dependent on its density according to

$$n_{air} - 1 = \kappa \cdot \rho, \qquad (1)$$

where ρ is the mean density ($\rho = 1.29$ kg/m^3) of air, and κ is the Gladstone-Dale coefficient ($\kappa = 2.3 \times 10^{-4}$ m^3/kg). Using the gas state equation

$$\rho = \frac{p}{R_s \cdot T}, \qquad (2)$$

where p is the atmospheric pressure, T is the absolute temperature, and R_s is the specific gas constant ($R_s = 287.06$ J/(kg·K) for air), the refractive index n_{air} is given by

$$(n_{air} - 1) = \frac{\kappa \cdot p}{R_s \cdot T} . \qquad (3)$$

It can further be shown that optical inhomogenities refract or bend light rays in proportion to their gradients of refractive index in an x, y-plane[12]. The resulting ray curvature is given by

$$\frac{\partial^2 x}{\partial z^2} = \frac{1}{n_{air}} \cdot \frac{\partial n_{air}}{\partial x} . \qquad (4)$$

Integrating once, the component of the angular ray deflection β_x in the x-direction is

$$\beta_x = \frac{1}{n_{air}} \cdot \int \frac{\partial n_{air}}{\partial x} \partial z. \qquad (5)$$

For schlieren of extent L along a path on the optical axis, Eq. (5) becomes

$$\beta_x = \frac{L}{n_{air}} \cdot \frac{\partial n_{air}}{\partial x} . \qquad (6)$$

Plugging in typical values for path lengths and gradients ($L = 300$ mm, $\ell = 50$ mm, the base length over which the assumed gradient is acting (see Fig. 2), $\Delta T = 1$ K, and $T = 300$ K), it results in a refraction angle

$$\beta_x = \frac{0.3}{1.00027 \cdot 0.05} \cdot \frac{2.3 \times 10^{-4} \cdot 1.01 \times 10^5}{287.06}$$
$$\cdot \left(\frac{1}{300} - \frac{1}{301} \right) \qquad (7)$$

of 5.4 μrad, which acts upon the assumed path length $L = 300$ mm, resulting in an deviation of Δx_a or Δx_b of around 1.6 μm; a way more than the resolution of the speckle system is sought.

An often overlooked factor influencing the systems uncertainty budget can be identified in the lack of pointing stability $\Delta \Theta$ of the laser source. A nice treatment on the subject can be found in Ref. [14] where also typical short- and long-term stability diagrams of HeNe lasers were discussed. The typical figures on pointing stability of a well known supplier of semiconductor lasers is to be found in Ref. [15]. To mention typical values given in the references $\Delta \Theta \leqslant 6$ μrad/K for a particular series of diode lasers[16] and $\Delta \Theta \leqslant 1.7$ μrad over approximately 1,000 s for well stabilized HeNe lasers[15]. If one again considers optical path lengths of 300 mm and 1 μrad results in a displacement figure for Δx_a or Δx_b of 0.3 μm, clearly a non-negligible term.

Since the generation of laser speckles can be thought of as being the action of light diffracted off of the superposition of randomly oriented diffraction gratings with random grating constants (the specimen surface), the effect a wavelength variation $\lambda \to \lambda + \Delta\lambda$ has is mainly a scaling of the speckle position with respect to the axis of the optical observing geometry[16]. If the geometry of the optical arrangement is such that the observation is perpendicular to the specimen surface and the pattern matching algorithm is tracking net speckle movement on average,

no directed displacement will be experienced. There is, however, an effect to increase the variance of the displacement estimation since with larger wavelength excursions $\Delta\lambda$, the patterns to match become increasingly dissimilar and noise artefacts prevail.

Yamaguchi has shown how to model the speckle pattern movements A_ξ and A_η (see Fig. 5) at the location of the camera as functions of various geometrical parameters[8]. These parameters comprise both rigid body translational (a_x, a_y, a_z) as well as rotational parameters $(\Omega_x, \Omega_y, \Omega_z)$ of the specimen about all three axes and also incorporating the non-ideal wavefronts of the laser source (by its radius of curvature ℓ_s). It is assumed that the optical axis of the camera is kept in a plane that is perpendicular to the specimen surface and that the viewed at specimen surface is parallel (to a very high degree) to the straining direction of the loading machine. Here, we define

$$\Omega = [\Omega_x, \Omega_y, \Omega_z]^{\mathrm{T}},$$
$$a = [a_x, a_y, a_z]^{\mathrm{T}},$$
$$\varepsilon = \begin{bmatrix} \varepsilon_{xx} & \varepsilon_{xy} \\ \varepsilon_{yx} & \varepsilon_{yy} \end{bmatrix},$$
$$\varepsilon_{xx} = \frac{\partial a_x}{\partial x}, \qquad \varepsilon_{yy} = \frac{\partial a_y}{\partial y},$$
$$A = [A_\xi, A_\eta]^{\mathrm{T}}. \tag{8}$$

Expressions of speckle shift values in straining direction A_ξ as well as the perpendicular direction A_η as seen by a camera placed the distance of $\updownarrow_0$ away from the specimen surface are given by

$$
\begin{aligned}
A_\xi = &\; a_x \cdot \left(\frac{\ell_0 \cdot \cos 2\vartheta_s}{\ell_s \cos \vartheta_0} + \cos \vartheta_0 \right) \\
&- a_z \cdot \left(\frac{\ell_0 \cos \vartheta_s \sin \vartheta_s}{\ell_s \cos \vartheta_0} + \sin \vartheta_0 \right) \\
&- \varepsilon_{xx} \cdot \ell_0 \cdot \left(\frac{\sin \vartheta_s}{\cos \vartheta_0} + \tan \vartheta_0 \right) \\
&+ \Omega_y \cdot \ell_0 \cdot \left(\frac{\cos \vartheta_s}{\cos \vartheta_0} + 1 \right), \\
A_\eta = &\; a_y \cdot \left(\frac{\ell_0}{\ell_s} + 1 \right) \\
&- \varepsilon_{xy} \cdot (\sin \vartheta_s + \sin \vartheta_0) \\
&- \Omega_x \cdot \ell_0 (\cos \vartheta_s + \cos \vartheta_0) \\
&- \Omega_z \cdot \ell_0 \cdot (\sin \vartheta_s + \sin \vartheta_0).
\end{aligned}
\tag{9}
$$

From these equations, one can derive the magnitude of possible strain/displacement measurement errors due to misalignment, rotations, and bending of the specimen during loading as well as those caused by non-collimated laser sources.

Again, as with the uncertainty contributions above, a numerical example consistent with the above assumptions shall be given here. Let's assume a radius of curvature $\ell_s = 1,500$ mm (this is a realistic assumption since for diode lasers for example, the laser light can savely be assumed to emanate from a point source at the laser diode location. The collimating optics attached to the laser does not change that fact much since the collimation
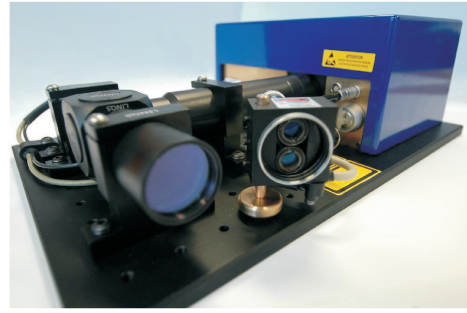

Fig. 3. Actual optical set-up of a speckle–correlation based strain measurement system.
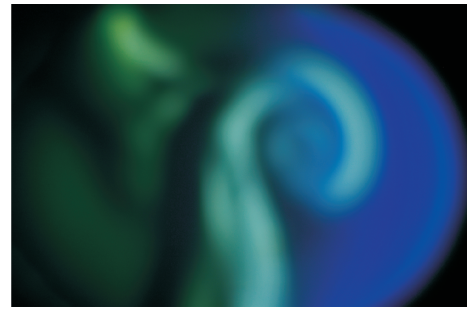

Fig. 4. Effect of light passing through an inhomogeneously dense volume of air clearly shows the schlieren effect. Shown here is the density and thus refractive index variation caused by unlit gas escaping from a cigarette lighter (not visible). The image was taken using an experimental schlieren system (from Ref. [13]).

needs to be set such as to average over the astigmatism of the beam), the projection distance $\ell_0 = 150$ mm, all angles being normal angles and a rigid body motion of the specimen in straining direction $a_x = 100$ μm (this assumption results from assuming a base length ℓ as seen in Fig. 2 of 50 mm and utilizing elastic strain values $(\varepsilon_{\max} = 2 \times 10^{-3})$). Then an error contribution for $\Delta A_\eta = a_x \cdot \ell_0/\ell_s = 10$ μm for a true value of 100 μm, a 10% error.

As might be inferred from Fig. 3, a typical system is built on an aluminum base with opto-mechanical components also made of black-anodized aluminum. This material as compared to stainless steel for example exhibits a rather large linear coefficient of thermal expansion $\alpha_{\mathrm{alu}} = 2.3 \times 10^{-5}$ K^{-1}. Again assuming sensible numbers on the heating up of the system during an experiment (2 K/min for example), and given a base plate to optical axis distance of 50 mm, an apparent movement of the specimen (as seen through a gradually thermally expanding optics) results in an error contribution Δx_a or Δx_b of $2.3 \times 10^{-5} \cdot 0.05 \cdot 2 = 2.3$ μm. Again an order of magnitude more than the resolution is sought.

To show how well corrected systems (the one shown in Fig. 3) might perfom, a short-term stability test is shown in Fig. 6. The laser source was a diode laser (warm-up time >2 h), the environmental conditions were that of a laboratory, five measurements per second were taken over a few minutes. Please note that the resolution as defined by the signal processing algorithm was deliberately set to 0.1 μm which is way below the short-term stability experienced.

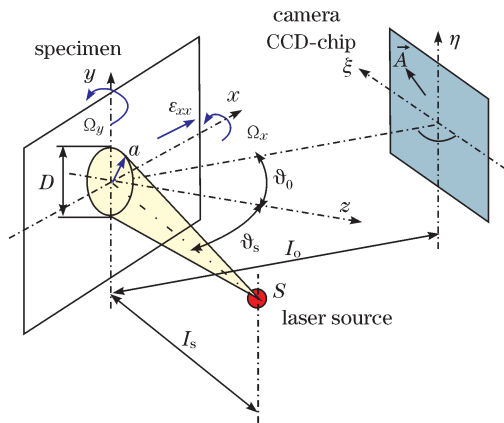Fig. 5. Definition of the geometry to derive laser speckle displacements A_ξ, A_η as seen by the camera.
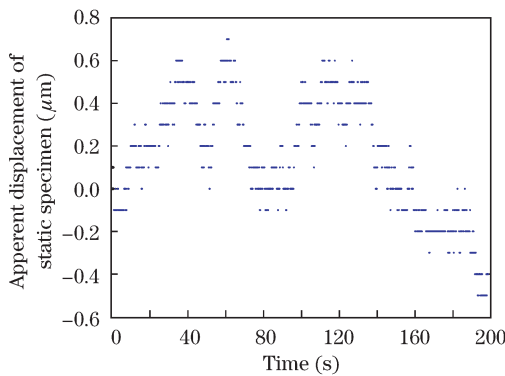

Fig. 6. Typical drift as seen in a laser-speckle system. The specimen was a copper slab mounted to a loading machine with no force applied. The measurement system was tightly locked to the base of the loading machine so as to circumvent differential motion and experiencing vibrations.

In conclusion, some easily overlooked sources of errors in laser-speckle systems (as well as many other optical systems) are discussed and it is shown that each and every error term can in the adverse case be orders of magnitude larger than the typical resolution that a user assumes from these systems. It might be concluded that the careful consideration of all types of influences is of utmost importance if uncertainties close to their theoret-ical limits are aimed for.

References

1. J. A. Jensen, *Estimation of Blood Velocities Using Ultrasound: A Signal Processing Approach* (Cambridge University Press, New York, 1996).

2. D. Massonnet and J.-C. Souyris, *Imaging with Synthetic Aperture Radar* (EPFL Press, Switzerland, 2008).

3. J. W. Goodman, *Speckle Phenomena in Optics* (Roberts and Company Publishers, Englewood, 2007).

4. R. Jones and C. Wykes, *Holographic and Speckle Interferometry* (Cambridge University Press, New York, 1989).

5. J. C. Dainty, *Laser Speckle and Related Phenomena* (Springer, Berlin, 1984).

6. G. H. Kaufmann, *Advances in Speckle Metrology and Related Techniques* (John Wiley and Sons Inc., Hoboken, 2011).

7. P. Rastogi, *Digital Speckle Pattern Interferometry and Related Techniques* (John Wiley and Sons Inc., Hoboken, 2000).

8. I. Yamaguchi, J. Mod. Opt. **28,** 1359 (1981).

9. R. K. Erf, *Speckle Metrology* (Academic Press Inc., San Diego, 1979).

10. S. C. Schneider, S. J. Rupitsch, and B. G. Zagar, IEEE Trans. Instrum. Meas. **56,** 2681 (2007).

11. S. C. Schneider, B. Zagar, and P. Zimprich, Technisches Messen **73,** 26 (2006).

12. G. S. Settles, *Schlieren and Shadowgraph Techniques-Visualizing Phenomena in Transparent Media* (Springer, Berlin, 2001).

13. D. Hofer and B. G. Zagar, in *Proceedings of 18th Symposium on Photonics in Measurements* (2008).

14. B. G. Zagar and R. Mittendorfer, in *Proceedings of International Conference on Computer Applications in Industry* 79 (1995).

15. J. Gray, P. Thomas, and X. D. Zhu, Rev. Sci. Instrum. **72,** 3714 (2001).

16. http://www.coherent.com/downloads.../CUBE_family_DSrevE_6.pdf.